Nanoparticle-macrophage interactions: A balance between clearance and cell-specific targeting

Rahul Rattan[a,c], **Somnath Bhattacharjee**[c], **Hong Zong**[c], **Corban Swain**[a,c], **Muneeb A. Siddiqui**[a,c], **Scott H. Visovatti**[a], **Yogendra Kanthi**[a,b], **Sajani Desai**[a,c], **David J. Pinsky**[a], and **Sascha N. Goonewardena**[a,b,c,*]

[a]Division of Cardiovascular Medicine, Internal Medicine, University of Michigan, Ann Arbor, MI, United States

[b]Ann Arbor Veterans Affairs Health System, Ann Arbor, MI, United States

[c]Michigan Nanotechnology Institute for Medicine and Biological Sciences, and Department of Internal Medicine, University of Michigan, Ann Arbor, MI 48109, United States

Abstract

The surface properties of nanoparticles (NPs) are a major factor that influences how these nanomaterials interact with biological systems. Interactions between NPs and macrophages of the reticuloendothelial system (RES) can reduce the efficacy of NP diagnostics and therapeutics. Traditionally, to limit NP clearance by the RES system, the NP surface is neutralized with molecules like poly(ethylene glycol) (PEG) which are known to resist protein adsorption and RES clearance. Unfortunately, PEG modification is not without drawbacks including difficulties with the synthesis and associations with immune reactions. To overcome some of these obstacles, we neutralized the NP surface by acetylation and compared this modification to PEGylation for RES clearance and tumor-specific targeting. We found that acetylation was comparable to PEGylation in reducing RES clearance. Additionally, we found that dendrimer acetylation did not impact folic acid (FA)-mediated targeting of tumor cells whereas PEG surface modification reduced the targeting ability of the NP. These results clarify the impact of different NP surface modifications on RES clearance and cell-specific targeting and provide insights into the design of more effective NPs.

1. Introduction

Because of their tunable physiochemical properties and enhanced carrying capacity, NPs have been used for a variety of biomedical applications.[1–3] Despite these advantages, many NPs have suffered setbacks because of their complex syntheses and our limited understanding of how NPs interact with biological systems. [4,5] Several variables can influence NP uptake including the size, shape, and surface charge.[6,7] It is known that positively charged NPs interact with the negatively charged phospholipid components of the cell membrane, increasing nonspecific interactions with biological cells and circulating

*Corresponding author at: University of Michigan Frankel Cardiovascular Center, 1500 East Medical Center Drive, SPC 5853, Ann Arbor, MI 48109-5853, United States. sngoonew@med.umich.edu (S.N. Goonewardena).

proteins.[6] Additionally, positively charged NP can also drive several undesirable biological responses including activation of the complement system, and increased cytotoxicity.[8–10] Recently it has been shown that electrostatic charge interactions between NP and cell membranes are convoluted with the protein corona effect, where the NP is enshrouded by protein macromolecules that results in non-specific interactions with cellular membranes.[11–13] This has been shown to increase NP clearance by macrophages of the RES, and decrease their downstream therapeutics.[14–17] The RES, an arm of the immune system consisting of phagocytic cells, can prevent the site-specific accumulation of NPs that is important for NP diagnostics and therapeutics. [18–21] Because of these undesirable effects, NP surfaces are typically neutralized. The impact of NP surface chemistry on NP-cell interactions has been broadly recognized.[6,22,23] Nevertheless, our understanding of how the physicochemical characteristics of NPs influence both clearance by the RES system and cell-specific targeting remains rather limited. A more complete understanding of NP characteristics and how they impact NP biological properties is necessary to more rationally design the next generation of NP diagnostics and therapeutics.

Dendrimers are branched NPs with a controllable chemical topology that have been used for molecular imaging and drug delivery.[24–26] Because of their low polydispersity and tunable chemical properties, dendrimers are well suited for mechanistic studies into NP interactions with biological systems.[27] In particular, poly(amido amine) (PAMAM) dendrimers have terminal amines that can be used to conjugate therapeutics, imaging agents, and other molecular payloads.[28–31] However, these terminal amines impart a positive charge to the dendrimer surface that can lead to the undesirable effects mentioned above. Because of these effects, like other NP, the dendrimer surface must be neutralized before being introduced into biological systems.

Surface attachment of hydrophilic oligomers such as poly(ethylene glycol) (PEG) to the dendrimer is one approach to neutralize its cationic surface. PEG conjugates are known to increase the circulating half-life of macromolecules by decreasing renal filtration, preventing opsonization, and reducing clearance by macrophages of the RES.[32–36] Although it is clear that PEGylation of NP can increase the circulating half-life and reduces RES clearance, PEGylation is not without drawbacks. PEG conjugates can generate an antibody response that can neutralize their efficacy upon chronic administration.[37–39] Furthermore, some studies have suggested that PEGylation can decrease NP uptake by target cells; this effect was attributed to increased steric hindrance due to the presence of PEG which prevents target moieties from binding to cell surface receptors.[40,41] To overcome some of these drawbacks, we explored acetylation to neutralize the surface of the NP as an alternative to PEGylation. Acetylation provides better control of the size and polydispersity of the NP compared with PEGylation given that any PEGylating agent is a polymer and inherently polydisperse.[42–44] Furthermore, because of the smaller size, we hypothesized that acetylation of the NP's surface would reduce macrophage clearance and would be less likely to interfere with cell-specific targeting of the NP.

Herein, we describe the synthesis of a suite of dendrimer NPs with different surface modifications to systematically evaluate acetylation with PEGylation and understand how these surface modifications affect NP clearance by the RES and tumor-specific targeting.

Building on our prior studies, we found that both acetylation and PEGylation of non-targeted PAMAM dendrimers reduce clearance by the RES.[45] Additionally, we demonstrate that acetylation of the targeted PAMAM dendrimers does not affect cell-specific targeting in a tumor cell model.

2. Materials and methods

2.1. Materials

All chemicals and materials were purchased from Sigma- Aldrich or Fisher Scientific and used as received unless otherwise specified. Both mPEG$_3$-NHS and mPEG$_7$-NHS were purchased from ChemPep (Wellington, FL). Phosphate buffer saline (PBS) without calcium and magnesium ions was purchased from Thermo Scientific (Logan, UT). The generation 5 poly(amidoamine) (G5 PAMAM) dendrimer was purchased from Dendritech and purified by dialysis (10K MWCO dialysis membrane) against PBS and H$_2$O. The 10K molecular weight cutoff (MWCO) centrifugal filters (Amicon Ultra-4) were purchased from Millipore (Billerica, MA). The 10K MWCO dialysis membrane was purchased from Spectrum Laboratories (Rancho Dominquez, CA).

KB and RAW264.7 cells were obtained from ATCC. RPMI media with L-Glutamine, RPMI without Folic acid (FA) and Penicillin/ Streptomycin (P/S) were obtained from Gibco. Fetal bovine serum (FBS) was obtained from Gemini Bio Products. Ultrapure 1 M Tris HCl pH 8.0, Alexa Flour 647 azide (AF647) and Prolong Golf with DAPI and 4 well Lab-Tek II chamber slide system were obtained from ThermoFisher Scientific, CuSO$_4$, and (+) Sodium L-ascorbate was obtained from Sigma-Aldrich. XTT cell viability kit was obtained from Cell Signaling Technology. Cells staining buffer (FACS buffer), Paraformaldehyde (PFA) and cell permeabilizing buffer (Saponin) was procured from BioLegend, Ted Pella INC and Sigma-Aldrich respectively.

2.2. Instruments

^{1}H NMR spectra were obtained using a Varian Inova 500 MHz. Electrospray ionization mass spectra (ESI-MS) were recorded using a Micromass Quattro II Electronic HPLC/MS/MS mass spectrometer. Analytical ultra-performance liquid chromatography (UPLC) was performed on a Waters Acquity Peptide Mapping System equipped with a photodiode array detector and an Acquity BEH C4 column (100×2.1 mm, 1.7 μm) at a flow rate of 0.21 mL/min. For analysis of the conjugates, a C5 silica-based RP-HPLC column (250×4.6 mm, 300 Å) connected to a C5 guard column (4×3 mm) was used. The mobile phase for elution of the conjugates was a linear gradient beginning with 100:0 (v/v) water/acetonitrile and ending with 20:80 (v/v) water/acetonitrile over 30 min at a flow rate of 1 mL/min. Trifluoroacetic acid (TFA) at 0.14 wt% concentration in water as well as in acetonitrile was used as a counter ion to make the dendrimer surfaces hydrophobic. FA-aN$_3$ (**5**) was synthesized as previously reported.[46]

2.3. Characterization of dendrimer conjugates

All the conjugates were analyzed by MALDI, UPLC and NMR, the methods of which have been previously described.[47–49]

2.4. Synthesis of G5-Alkyne-NH$_2$ (1)

Conjugates were prepared using G5 via EDC-NHS coupling. In brief, amine-terminated monomer G5 (400.0 mg, 0.0152 mmol) was dissolved in deionized water (4 mL). 4-(2-Propyn-1-yloxy)- Benzenepropanoic acid (62.0 mg, 0.304 mmol) was activated by dissolving in 4 mL acetonitrile with *N*-(3-Dimethylaminopropyl)- N′-ethylcarbodiimide hydrochloride (EDC) (116.5 mg, 0.608 mmol) and *N*-hydroxysuccinimide (NHS) (70.0 mg, 0.608 mmol) and stirred for 3 h. The activated alkyne linker solution was added drop wise to the dendrimer solution and allowed to stir overnight. The product was purified using Amicon Ultra Centrifugal units, 10 kDa MWCO membranes, 5 PBS washes, and 5 DI washes. A total of 432.6 mg of white solid was isolated via lyophilization.

2.5. Synthesis of G5-Alkyne-NHAc (2)

1 (120.0 mg, 4.29 μmol) was fully acetylated (100% of remaining primary amines converted to acetyl groups) by re-dissolving in anhydrous methanol (20.0 mL), adding 150 equiv. of triethylamine (TEA) and 150 equiv. of acetic anhydride (Ac$_2$O), and stirring for 4 h. The product was purified using Amicon Ultra Centrifugal units, 10 kDa MWCO membranes, 5 PBS washes, and 5 DI washes. A total of 100.2 mg of **2** as a white solid was isolated via lyophilization.

2.6. Synthesis of G5-Alkyne-PEG$_3$ (3)

1 (20.0 mg, 0.714 μmol) and DIPEA (13.8 mg, 0.107 mmol) were dissolved in anhydrous DMSO (1.0 mL). A mPEG$_3$-NHS (120.0 mg, 0.360 mmol) DMSO (1.0 mL) solution was added drop wise. The reaction mixture was stirred at room temperature for an additional 24 h. The product was purified using Amicon Ultra Centrifugal units, 10 kDa MWCO membranes, 5 PBS washes, and 5 DI washes. A total of 22.5 mg of **3** as a white solid was isolated via lyophilization.

2.7. Synthesis of G5-Alkyne-PEG$_7$ (4)

1 (20.0 mg, 0.714 μmol) and DIPEA (13.8 mg, 0.107 mmol) were dissolved in anhydrous DMSO (1.0 mL). An mPEG$_7$-NHS (182.0 mg, 0.360 mmol) DMSO (1.0 mL) solution was added drop wise. The reaction mixture was stirred at room temperature for an additional 24 h. The product was purified using Amicon Ultra Centrifugal units, 10 kDa MWCO membranes, 5 PBS washes, and 5 DI washes. A total of 25.1 mg of **4** as a white solid was isolated via lyophilization.

2.8. Synthesis of G5-Alkyne-FA-NH$_2$ (5)

1 (60.0 mg, 2.14 μmol) was dissolved in Cu(II) sulfate (10 mol% per compound **9**, 1 mg/mL H$_2$O) and sodium ascorbate (60 mol% per compound **9** 1 mg/mL H$_2$O solution) solution. Compound **9** (7.5 mol ratio to G5-Alkyne-NH$_2$ **1**, 10 mg/mL DMSO solution) was added. The reaction mixture was stirred at room temperature under N$_2$ overnight. Samples were purified using 10 kDa MWCO centrifugal filtration devices. Purification consisted of ten cycles (20 min at 4800 rpm) using PBS (5 cycles) and DI water (5 cycles). A total of 62.2 mg of **5** as a brown solid was isolated via lyophilization.

2.9. Synthesis of G5-Alkyne-FA-NHAc (6)

5 (15.0 mg, 0.455 μmol) was dissolved in anhydrous methanol (1.0 mL), adding 150 equiv. of triethylamine (TEA) and 150 equiv. of acetic anhydride (Ac_2O), and stirred for 4 h. The product was purified using Amicon Ultra Centrifugal units, 10 kDa MWCO membranes, 5 PBS washes, and 5 DI washes. A total of 14.6 mg of **6** as a brown solid was isolated via lyophilization.

2.10. Synthesis of G5-Alkyne-FA-PEG$_3$ (7)

5 (10.0 mg, 0.333 μmol) and trimethylamine (13.4 mg, 0.132 mmol) were dissolved in anhydrous DMSO (400 μL). The mPEG$_3$-NHS (44.4 mg, 0.133 mmol) DMSO (100 μL) solution was added drop wise. The reaction mixture was stirred at room temperature overnight. The product was purified using Amicon Ultra Centrifugal units, 10 kDa MWCO cutoff membranes, 5 PBS washes, and 5 DI washes. A total of 10.9 mg of **7** as a brown solid was isolated via lyophilization.

2.11. Synthesis of G5-Alkyne-FA-PEG$_7$ (8)

5 (10.0 mg, 0.333 μmol) and trimethylamine (13.4 mg, 0.132 mmol) were dissolved in anhydrous DMSO (400 μL). The mPEG$_7$-NHS (68.0 mg, 0.133 mmol) DMSO (100 μL) solution was added drop wise. The reaction mixture was stirred at room temperature overnight. The product was purified using Amicon Ultra Centrifugal units, 10 kDa MWCO membranes, 5 PBS washes, and 5 DI washes. A total of 11.9 mg of **8** as a brown solid was isolated via lyophilization.

2.12. Zeta potential

Zeta Potential (ZP) measurements were performed using DTS- 1070 cuvette in Zetasizer Nano-ZS (Malvern Instruments Ltd). For ZP measurements, surface modified NP **1**–**4** were diluted to 5 μM in molecular grade water and 1 mM HEPES buffer with pH 7.0. These dilutions were made at RT, and 5 min before measurement. Error for ZP measurements was reported as actual measurement zeta deviation values.

2.13. Cell culture

To evaluate the biological effects of NP surface modifications, two cell models were employed. RAW264.7 cells, macrophage cell model, was used to evaluate RES interactions.[50,51] KB cells, a tumor cell model that overexpresses the Folic acid receptor, were used to evaluate cell-specific targeting.[52–54] KB and RAW264.7 were maintained at 37 °C in a 5% CO_2 humidified incubator. RPMI without FA with 10% FBS and 1% P/S and RPMI with L-Glutamine and 10% FBS and 1% P/S was used for KB and RAW264.7 cells respectively. For flow cytometry cells were plated in a 24-well plate. For cytotoxicity assays, cells were plated in 96-well plate. For confocal microscopy studies, cells were plated in 4 well Lab-Tek II Chamber slide system. Cells were allowed to attach overnight at 37 °C before use. Prior to flow cytometry analysis, RAW264.7 cells were washed twice with FACS buffer. 500 μL of cell staining buffer was then added to each well, and a cell scraper was used to dissociate cells from the surface.[55,56] The resulting cell suspension was then

transferred to 1.5 mL Eppendorf tubes and centrifuged at 1200 rpm for 5 min at 4 °C. The supernatant was removed and the pellet was suspended in FACS buffer.

Prior to flow cytometry analysis of KB cells, KB cells were washed twice with FACS buffer and once with PBS without Ca^{2+} and Mg^{2+}. 200 μL of trypsin was then added to each well and incubated for 5 min at 37 °C and 5% CO_2.[57] 800 μL of KB media was then added to each well containing now dissociated cells. The resulting cell suspension was then transferred to 1.5 mL Eppendorf tubes and centrifuged at 1200 rpm for 5 min at 4 °C. The supernatant was removed and the pellet was suspended in FACS buffer.

2.14. Cytotoxicity assays

For cell viability study, cell treatment was done with 100 nM conjugates **1**–**4** for 2, 24, and 48 h. XTT cell cytotoxicity assay were performed as per the company's prescribed procedure.[58–60] All measurements were done in triplicates and the compiled data is presented as mean fluorescent units ± standard deviation.

2.15. Flow cytometry in-situ click reaction (CuAAC reaction)

For flow cytometry, cell treatment was done with 10 nM conjugates for 2 h. Cells were washed and pelleted as described above. The cell pellets were fixed with 4% PFA and permeabilized with 1× Saponin prior to in situ CuAAC reaction. Fluorescent AF647 azide was reacted with dendrimer conjugates for 1 h with Tris (100 mM, pH 8.5), $CuSO_4$ (1 mM), AF647 azide (100 μM) and L-ascorbic acid (100 mM). After staining the cells were washed once with 1× Saponin solution and twice with FACS buffer. Cells were resuspended in FACS buffer and flow cytometry was performed.

2.16. Confocal microscopy CuAAC reaction

For confocal microscopy, cell treatment was done with 100 nM conjugates for 2 h. Cells were plated in 4 well Lab-Tek II Chamber slides and were treated with the dendrimer conjugates at 37 °C, 5% CO_2 for 2 h. After incubation, the cells were washed twice with FACS buffer, then fixed with 4% PFA and permeabilized with 0.25% Triton-X100 for 20 min. The in situ CuAAC reaction was performed on the slides using a similar CuAAC protocol as described above except using fluorescent AF555 azide. After the reaction, the cells were washed once with TritonX-100 and twice with FACS buffer. Prolong gold containing DAPI was then added to the cells and the slide was covered with #1.5 cover glass. Slide was stored at 4 °C until confocal was performed. Confocal images were obtained on a Leica Inverted SP5X confocal microscope using a 1.25 NA oil immersion objective. To visualize DAPI, the 405 diode laser was used for excitation, and the emission was filtered at 412–475 nm. To visualize AF555, the 519 nm line of the Argon laser was used for excitation, and the emission was filtered at 531–719 nm.

Isolated products were first characterized by ^{1}H-NMR (Figure S1) using D_2O as a solvent and water peak at 4.70 ppm as a reference. Two broad singlets appeared for compounds **1**–**8** around 6.8 and 7.1 ppm correspond to aromatic protons of the attached alkyne. We also observed two broad singlets at 7.5 and 7.8 ppm that correspond to the aromatic protons of

2.17. Statistical analysis

For flow cytometry all measurements were done in triplicate. The data is presented as mean fluorescent units ± standard deviation. Significant differences between group means were evaluated using one-way Anova, Dunnett's post hoc test, P value < 0.05. The analysis was performed using GraphPad Prism (GraphPad Software, Inc.; La Jolla, CA)

3. Results

3.1. Synthesis and Characterization of dendrimer conjugates

We synthesized targeted (FA-modified) and non-targeted dendrimer (without FA) conjugates as illustrated in Scheme 1. In brief, G5-Alkyne-NH_2 (**1**) was synthesized by reacting G5 with 4-(2-propyn-1-yloxy)-benzenepropanoic acid in presence of *N*-Hydroxysuccinimide (NHS) and 1-Ethyl-3-(3-dimethylaminopropyl) carbodiimide (EDC) at room temperature and pure compound **1** was isolated by ultracentrifugation employing Amicon Ultra Centrifugal Filters. Isolated compound **1** was further reacted with acetic anhydride or PEG_m-NHS (m = 3 and 7) in order to neutralize the primary amines to yield desired compounds **2**, **3**, and **4** respectively. Next, we synthesized FA-N_3 (**9**) as previously described.[61] Subsequently, we synthesized the targeted (FA-modified) dendrimer conjugates **5**–**8**. First, we synthesized G5-alkyne-FA-NH_2 (**5**) employing click chemistry in the presence of $CuSO_4$ and sodium ascorbate between compounds **1** and **9**. Compound **5** was further reacted with acetic anhydride or PEG_m-NHS (m = 3 and 7) to prepare conjugates **6**–**8** respectively. After each step, intermediates were purified by centrifugal ultrafiltration. The final products were characterized by ^{1}H NMR, UPLC and MALDI.

Isolated products were first characterized by ^{1}H NMR (Fig. S1) using D_2O as a solvent and water peak at 4.70 ppm as a reference. Two broad singlets appeared for compounds **1**–**8** around 6.8 and 7.1 ppm correspond to aromatic protons of the attached alkyne. We also observed two broad singlets at 7.5 and 7.8 ppm that correspond to the aromatic protons of the conjugated folic acid derivatives for compounds **5**–**8**. ^{1}H NMR of compounds **7** and **8** showed broad singlets from 3.49 to 3.72 ppm that correspond to —CH_2CH_2O and —OCH_3 of PEG respectively. Singlets appeared for compounds **2** and **6** at 1.9 ppm correspond to CH_3CONH—. Conjugates and intermediates were also analyzed by Ultra Performance Liquid Chromatography (UPLC) and matrix assisted laser desorption ionization/time-of-flight mass spectrometry (MALDI-TOF MS). Fig. S2 (shown in supporting information) illustrates UPLC chromatogram of PAMAM dendrimer conjugates. The peaks corresponding to isolated pure compounds (**1**–**8**) appear as single peak. The conjugates were further characterized by MALDI-TOF MS (Fig. S3) and average MWs of conjugates were calculated.

3.2. Surface Characterization and cytotoxicity of dendrimer conjugates

After synthesizing the dendrimer conjugates, we sought to evaluate the surface charge and cytotoxicity of the dendrimer conjugates **1**–**4**, both of which would could impact NP specificity and efficacy. It has already been demonstrated that cationic NPs have nonspecific interactions with circulating proteins and cells and can also induce cytotoxicity.[62] Because it is clear that the surface charge of nanoparticles can greatly affect their biological properties,

we determined the zeta potential of the dendrimer conjugates. Consistent with prior reports, the unmodified G5 dendrimer (**1**) had the highest positive charge of all conjugates tested while the surface neutralized dendrimers (**2–4**) were close to neutral in both molecular grade water and 1 mM HEPES pH 7 buffer (Fig. 1) To assess the cytotoxicity of these dendrimer conjugates, the suite of dendrimers were incubated with RAW264.7 cells. We used RAW264.7 cells, a murine macrophage cell line, as a cell model of the RES as has been extensively reported.[63–66] Cell cytotoxicity was measured using the XTT assay as we have previously reported.[67,68] At 100 nM concentration, none of the dendrimer conjugates **1–4** showed evidence of cytotoxicity (Fig. 2).

3.3. RES clearance of the dendrimer conjugates

After evaluating the cytotoxicity and charge properties of the dendrimer conjugates, we then sought to examine how the NP surface modifications affected NP clearance by RES cells. To examine NP clearance, we took advantage of our recently developed NP tracking technique which relies upon an in situ bioorthogonal click reaction with a fluorophore allowing us to track NP cellular uptake.[69] The technique is based on a Copper (I) based Huisgen cycloaddition reaction where, with the help of Cu (I) as catalyst, the alkyne handle on the NP is covalently clicked onto the azide handle on the fluorophore post cellular uptake.[70] This technique greatly simplifies the biological evaluation of NP in that it does not require additional functionalization of the various NP with fluorophores before their use in biological systems. RAW264.7 cells, RES model system, were incubated with 10 nM and 100 nM of the dendrimer conjugates for flow cytometry and confocal microscopy respectively, and uptake was examined at 2 h using our in situ tracking technique.[51] After incubation, the cells were processed and AF647 (for flow cytometry) or AF555 (for confocal microscopy) was conjugated to the internalized dendrimer conjugates using the CuAAC reaction. As shown in Fig. 3, the two PEGylated conjugates (**3** and **4**) and acetylated (**2**) dendrimer conjugates were not cleared by RAW264.7 compared with the non-modified, amine-terminated dendrimer scaffold (**5**) (one way ANOVA, Dunnett's post hoc test, $p < 0.05$). These results suggest that acetylation of dendrimer conjugates functions similarly to PEGylation with respect to minimizing RES clearance of NP. RES clearance of the targeted conjugates is shown in Fig. S4, like the non-targeted version the targeted G5-Alkyne-FA-NHAc (**6**), G5-Alkyne-FA-PEG$_3$ (**7**), and G5-Alkyne-FA-PEG$_7$ (**8**) show minimal RES clearance. These results suggest that acetylated dendrimers reduces RES clearance similar to that of PEGylated dendrimers.

3.4. Effects of surface modification on tumor-specific targeting

After confirming that acetylated and PEGylated dendrimer surface is similar in reducing clearance by macrophages, we sought to evaluate its effects on cell-specific targeting. We employed KB cells, a tumor-cell model that overexpresses the folate receptor, to evaluate cell-specific targeting of the dendrimer conjugates.[52,53] KB cells were incubated with 10 nM of the FA-targeted dendrimer conjugates **5–8** and uptake was examined at 2 h using our in situ tracking technique. After incubation, the cells were processed and AF647 was conjugated to the internalized FA-targeted dendrimer conjugates using the CuAAC reaction and then assessed by flow cytometry. As expected, all FA-targeted dendrimer conjugates show increased uptake compared with vehicle controls (Fig. 4). Interestingly, the acetylated

G5-FA (**6**) shows higher uptake than that of the PEGylated dendrimer conjugates **7** and **8** (one way ANOVA, Dunnett's post hoc test, p < 0.05). These results suggest that acetylation of dendrimer conjugates have less of a detrimental effect on cell-specific targeting compared with PEGylated dendrimer conjugates. More importantly, in essence PEGylation should increase the solubility and acetylation should reduce solubility of macromolecules in water. However, no solubility related problem was observed due to the acetylation of dendrimer in the preparation of aqueous solution. Moreover, higher uptake was shown in both macrophages and the tumor cell model by **6** than **7** and **8** further indicates that no adverse effect due to any change of solubility by acetylation of dendrimer. Additionally, Fig. S5 shows KB uptake for non-targeted conjugates, G5-Alkyne-NHAc (**2**), G5-Alkyne-PEG$_3$ (**3**), G5-Alkyne-PEG$_7$ (**4**) show minimal uptake; these results confirm that FA is important for NP internalization by KB cells. Additionally, it also shows that targeted acetylated (**6**) and PEGylated (**7** and **8**) NP uptake was facilitated by FA targeting.

4. Discussion

In this study, we engineered a suite of dendrimer conjugates and systematically evaluated how distinct surface modifications affected NP clearance by the RES and tumor-specific targeting. We found that 1) both acetylation and PEGylation of the dendrimer surface reduces clearance by the RES system and 2) that PEGylation of FA-targeted dendrimers reduces tumor-specific targeting while acetylation of FA-targeted dendrimers does not negatively impact tumor-specific targeting (Fig. 5).

One of the major barriers limiting nanotherapeutic delivery is an inability to attain therapeutic levels at the target tissue because of NP clearance by the RES. The RES system, which consists predominantly of macrophages, functions to sequester and clear NP after their administration.[71] To improve NP circulating half-life and to reduce NP clearance by the RES system, PEGylation has been widely used in drug delivery.[72,73] However, several recent studies have suggested that PEGylation can have some detrimental effects on NP including those on the NP therapeutic index and possibly triggering immune reactions.[38,74–76] Another practical limitation of PEGylating NPs is that the synthesis and purification can be more difficult as PEG molecules are inherently polydisperse and the addition PEG molecules can lead to batch-to-batch variability.[77]

To overcome some of the limitations of PEGylation, several studies have explored alternatives.[78][79–81] Mantovani et al. presented *N*-maleimido-functionalized polymers as an alternative to PEGylation; major drawbacks of this work is that reaction between two macromolecules involve separate synthesis and attachment of a polymer to another macromolecule, often suffer from low yield due to steric hindrance and difficulty in product purification as a result of similar sizes and surface properties of the reactants and products.[82] Additionally, Estephan and colleagues presented a zwitterionic alternative to PEGylation.[83] This study was particularly interesting as it provided the advantages of PEG without adding steric hindrance to the nanoparticle which PEG does; however the study lacked *in vitro* cancer cell experiments.

In this study, we found that acetylation functions similarly to PEGylation with respect to reducing RES clearance; interestingly, we also found that acetylated dendrimers did not reduce tumor-specific targeting compared with PEGylated dendrimers. We hypothesize that acetylated dendrimers reduce RES clearance by neutralizing the cationic surface of the dendrimer and reducing electrostatic interactions with serum proteins and cell membranes; this is supported by the data as positively charged dendrimers demonstrate higher RES clearance. We believe that the higher targeted uptake of acetylated dendrimer compared with PEGylation reflects a reduced steric hindrance between FA and the folate receptor with the acetylated dendrimer conjugates. Acetylation as surface modification is not only applicable to dendrimers but also potentially applicable to other NP therapeutics and imaging agents.[84,85] Moreover, acetylation can also provide for better control for the size and polydispersity of the NP compared to PEGylation.[86,87]

Although we believe that the findings of this study will help us to better understand NP-RES interactions, several limitations warrant consideration. The NP surface modifications were only evaluated with one receptor ligand system, and only in cell models. Additionally, studies are ongoing to validate these findings with other receptor-ligand systems and *in vivo* to further examine the full potential of acetylation as a viable alternative to PEGylation of NPs.

5. Conclusion

In summary, this study demonstrates that acetylation is an effective alternative to PEGylation for NP surface modification in that it 1) reduces clearance by RES cells and 2) it does not affect tumor-specific targeting. We believe these results clarify the biological impact of different NP surface modifications and provide insights that could help to design of more effective NPs.

Supplementary Material

Refer to Web version on PubMed Central for supplementary material.

Acknowledgments

References

1. Leuschner F, Dutta P, Gorbatov R, et al. Therapeutic sirna silencing in inflammatory monocytes. Nat Biotechnol. 2011; 29:1005–1010. [PubMed: 21983520]

2. Nam J-M, Thaxton CS, Mirkin CA. Nanoparticle-based bio-bar codes for the ultrasensitive detection of proteins. Science. 2003; 301:1884–1886. [PubMed: 14512622]

3. Tsapis N, Bennett D, Jackson B, Weitz DA, Edwards DA. Trojan particles: large porous carriers of nanoparticles for drug delivery. Proc Natl Acad Sci USA. 2002; 99:12001–12005. [PubMed: 12200546]

4. Duncan R, Gaspar R. Nanomedicine(S) under the microscope. Mol Pharm. 2011; 8:2101–2141. [PubMed: 21974749]

5. Ornelas C, Broichhagen J, Weck M. Strain-promoted alkyne azide cycloaddition for the functionalization of poly(amide)-based dendrons and dendrimers. J Am Chem Soc. 2010; 132:3923–3931. [PubMed: 20184364]

6. Verma A, Stellacci F. Effect of surface properties on nanoparticle-cell interactions. Small. 2010; 6:12–21. [PubMed: 19844908]

7. Cho EC, Au L, Zhang Q, Xia Y. The effects of size, shape, and surface functional group of gold nanostructures on their adsorption and internalization by cells. Small. 2010; 6:517–522. [PubMed: 20029850]

8. Toda M, Iwata H. Effects of hydrophobicity and electrostatic charge on complement activation by amino groups. ACS Applied Materials & Interfaces. 2010; 2:1107–1113. [PubMed: 20380387]

9. Fornaguera C, Caldero G, Mitjans M, Vinardell MP, Solans C, Vauthier C. Interactions of Plga nanoparticles with blood components: protein adsorption, coagulation, activation of the complement system and hemolysis studies. Nanoscale. 2015; 7:6045–6058. [PubMed: 25766431]

10. Dobrovolskaia MA, Aggarwal P, Hall JB, McNeil SE. Preclinical studies to understand nanoparticle interaction with the immune system and its potential effects on nanoparticle biodistribution. Mol Pharm. 2008; 5:487–495. [PubMed: 18510338]

11. Forest V, Cottier M, Pourchez J. Electrostatic interactions favor the binding of positive nanoparticles on cells: a reductive theory. Nano Today. 2015; 10:677–680.

12. Corbo C, Molinaro R, Parodi A, Toledano Furman NE, Salvatore F, Tasciotti E. The impact of nanoparticle protein corona on cytotoxicity. Immunotoxicity and target drug delivery. Nanomedicine. 2015; 11:81–100. [PubMed: 26653875]

13. Lundqvist M, Stigler J, Elia G, Lynch I, Cedervall T, Dawson KA. Nanoparticle size and surface properties determine the protein corona with possible implications for biological impacts. Proc Natl Acad Sci. 2008; 105:14265–14270. [PubMed: 18809927]

14. Agashe HB, Dutta T, Garg M, Jain NK. Investigations on the toxicological profile of functionalized fifth-generation poly(propylene imine) dendrimer. J Pharm Pharmacol. 2006; 58:1491–1498. [PubMed: 17132212]

15. Roberts JC, Bhalgat MK, Zera RT. Preliminary biological evaluation of polyamidoamine (pamam) starbursttm dendrimers. J Biomed Mater Res. 1996; 30:53–65. [PubMed: 8788106]

16. Malik N, Wiwattanapatapee R, Klopsch R, et al. Dendrimers: relationship between structure and biocompatibility in vitro, and preliminary studies on the biodistribution of 125i-labelled polyamidoamine dendrimers in vivo. J Control Release. 2000; 65:133–148. [PubMed: 10699277]

17. Bhattacharjee S, Liu W, Wang W-H, et al. Site-specific zwitterionic polymer conjugates of a protein have long plasma circulation. ChemBioChem. 2015; 16:2451–2455. [PubMed: 26481301]

18. Panyam J, Labhasetwar V. Biodegradable nanoparticles for drug and gene delivery to cells and tissue. Adv Drug Deliv Rev. 2003; 55:329–347. [PubMed: 12628320]

19. Owens DE III, Peppas NA. Opsonization, biodistribution, and pharmacokinetics of polymeric nanoparticles. Int J Pharm. 2006; 307:93–102. [PubMed: 16303268]

20. Wang AZ, Langer R, Farokhzad OC. Nanoparticle delivery of cancer drugs. Annu Rev Med. 2012; 63:185–198. [PubMed: 21888516]

21. Walkey CD, Olsen JB, Guo H, Emili A, Chan WCW. Nanoparticle size and surface chemistry determine serum protein adsorption and macrophage uptake. J Am Chem Soc. 2012; 134:2139–2147. [PubMed: 22191645]

22. Nel AE, Madler L, Velegol D, et al. Understanding biophysicochemical interactions at the nano-bio interface. Nat Mater. 2009; 8:543–557. [PubMed: 19525947]

23. Albanese A, Tang PS, Chan WCW. The effect of nanoparticle size, shape, and surface chemistry on biological systems. Annu Rev Biomed Eng. 2012; 14:1–16. [PubMed: 22524388]

24. Lee CC, MacKay JA, Frechet JMJ, Szoka FC. Designing dendrimers for biological applications. Nat Biotechnol. 2005; 23:1517–1526. [PubMed: 16333296]

25. Stiriba S-E, Frey H, Haag R. Dendritic polymers in biomedical applications: from potential to clinical use in diagnostics and therapy. Angew Chem Int Ed. 2002; 41:1329–1334.

26. Svenson S, Tomalia DA. Dendrimers in biomedical applications-reflections on the field. Adv Drug Delivery Rev. 2005; 57:2106–2129.

27. Najlah M, D'Emanuele A. Crossing cellular barriers using dendrimer nanotechnologies. Curr Opin Pharmacol. 2006; 6:522–527. [PubMed: 16890022]

28. Morgan MT, Carnahan MA, Immoos CE, et al. Dendritic molecular capsules for hydrophobic compounds. J Am Chem Soc. 2003; 125:15485–15489. [PubMed: 14664594]

29. Wang Y, Guo R, Cao X, Shen M, Shi X. Encapsulation of 2-methoxyestradiol within multifunctional poly(amidoamine) dendrimers for targeted cancer therapy. Biomaterials. 2011; 32:3322–3329. [PubMed: 21315444]

30. Kong L, Alves CS, Hou W, et al. Rgd peptide-modified dendrimer-entrapped gold nanoparticles enable highly efficient and specific gene delivery to stem cells. ACS Appl Mater Interfaces. 2015; 7:4833–4843. [PubMed: 25658033]

31. Dufes C, Uchegbu IF, Schaetzlein AG. Dendrimers in gene delivery. Adv Drug Delivery Rev. 2005; 57:2177–2202.

32. Caliceti P, Veronese FM. Pharmacokinetic and biodistribution properties of poly (ethylene glycol)-protein conjugates. Adv Drug Delivery Rev. 2003; 55:1261–1277.

33. van Vlerken L, Vyas T, Amiji M. Poly(ethylene glycol)-modified nanocarriers for tumor-targeted and intracellular delivery. Pharm Res. 2007; 24:1405–1414. [PubMed: 17393074]

34. Perry JL, Reuter KG, Kai MP, et al. Pegylated print nanoparticles: the impact of peg density on protein binding, macrophage association, biodistribution, and pharmacokinetics. Nano Lett. 2012; 12:5304–5310. [PubMed: 22920324]

35. Saha K, Rahimi M, Yazdani M, et al. Regulation of macrophage recognition through the interplay of nanoparticle surface functionality and protein corona. ACS Nano. 2016

36. Schöttler S, Becker G, Winzen S, et al. Protein adsorption is required for stealth effect of poly(ethylene glycol)- and poly(phosphoester)-coated nanocarriers. Nat Nano. 2016; 11:372–377.

37. Ishida T, Masuda K, Ichikawa T, Ichihara M, Irimura K, Kiwada H. Accelerated clearance of a second injection of pegylated liposomes in mice. Int J Pharm. 2003; 255:167–174. [PubMed: 12672612]

38. Ishida T, Wang X, Shimizu T, Nawata K, Kiwada H. Pegylated liposomes elicit an anti-peg igm response in a T cell-independent manner. J Control Release. 2007; 122:349–355. [PubMed: 17610982]

39. Mima Y, Hashimoto Y, Shimizu T, Kiwada H, Ishida T. Anti-Peg IgM is a major contributor to the accelerated blood clearance of polyethylene glycol-conjugated protein. Mol Pharm. 2015; 12:2429–2435. [PubMed: 26070445]

40. Kubetzko S, Sarkar CA, Pluckthun A. Protein pegylation decreases observed target association rates via a dual blocking mechanism. Mol Pharmacol. 2005; 68:1439–1454. [PubMed: 16099846]

41. Harris JM, Martin NE, Modi M. Pegylation. Clin Pharmacokinet. 2012; 40:539–551.

42. Veronese FM, Pasut G. Pegylation, successful approach to drug delivery. Drug Discovery Today. 2005; 10:1451–1458. [PubMed: 16243265]

43. Gaberc-Porekar V, Zore I, Podobnik B, Menart V. Obstacles and pitfalls in the pegylation of therapeutic proteins. Curr Opin Drug Discov Devel. 2008; 11:242–250.

44. Veronese FM. Peptide and protein pegylation: a review of problems and solutions. Biomaterials. 2001; 22:405–417. [PubMed: 11214751]

45. Quintana A, Raczka E, Piehler L, et al. Design and function of a dendrimer-based therapeutic nanodevice targeted to tumor cells through the folate receptor. Pharm Res. 2002; 19:1310–1316. [PubMed: 12403067]

46. Goonewardena SN, Kratz JD, Zong H, et al. Design considerations for pamam dendrimer therapeutics. Bioorg Med Chem Lett. 2013; 23:2872–2875. [PubMed: 23583511]

47. Majoros IJ, Thomas TP, Mehta CB, Baker JR. Poly(amidoamine) dendrimer-based multifunctional engineered nanodevice for cancer therapy. J Med Chem. 2005; 48:5892–5899. [PubMed: 16161993]

48. Mullen DG, Fang M, Desai A, Baker JR, Orr BG, Holl MMB. A quantitative assessment of nanoparticle-ligand distributions: implications for targeted drug and imaging delivery in dendrimer conjugates. ACS Nano. 2010; 4:657–670. [PubMed: 20131876]

49. Zong H, Thomas TP, Lee KH, et al. Bifunctional pamam dendrimer conjugates of folic acid and methotrexate with defined ratio. Biomacromolecules. 2012; 13:982–991. [PubMed: 22360561]

50. Tacchini L, Gammella E, De Ponti C, Recalcati S, Cairo G. Role of Hif-1 and Nf-κb transcription factors in the modulation of transferrin receptor by inflammatory and anti-inflammatory signals. J Biol Chem. 2008; 283:20674–20686. [PubMed: 18519569]

51. Xia, W., Song, H-M., Wei, Q., Wei, A. Differential response of macrophages to core-shell Fe(3)O(4)@Au nanoparticles and nanostars; Nanoscale. 2012. p. 4http://dx.doi.org/10.1039/c1032nr32070c

52. Bae Y, Jang WD, Nishiyama N, Fukushima S, Kataoka K. Multifunctional polymeric micelles with folate-mediated cancer cell targeting and Ph-triggered drug releasing properties for active intracellular drug delivery. Mol BioSyst. 2005; 1:242–250. [PubMed: 16880988]

53. Zwicke, GL., Mansoori, GA., Jeffery, CJ. Utilizing the folate receptor for active targeting of cancer nanotherapeutics; Nano Rev. 2012. p. 3http://dx.doi.org/10.3402/nano.v3403i3400.18496

54. Liu T, Choi H, Zhou R, Chen IW. Quantitative evaluation of the reticuloendothelial system function with dynamic Mri. PLoS One. 2014; 9:e103576. [PubMed: 25090653]

55. Jacobs AT, Ignarro LJ. Lipopolysaccharide-induced expression of interferon-β mediates the timing of inducible nitric-oxide synthase induction in raw 264.7 macrophages. J Biol Chem. 2001; 276:47950–47957. [PubMed: 11602590]

56. Ishii R, Horie M, Saito K, Arisawa M, Susumu K. Inhibitory effects of phloroglucinol derivatives from Mallotus japonicus on nitric oxide production by a murine macrophage-like cell line, raw 264.7, activated by lipopolysaccharide and interferon-Γ. Biochim Biophys Acta Gen Subj. 2001; 1568:74–82.

57. Klement V, McAllister RM. Syncytial cytopathic effect in Kb cell of a C-type RNA virus isolated from human rhabdomyosarcoma. Virology. 1972; 50:305–308. [PubMed: 4343115]

58. Scudiero DA, Shoemaker RH, Paull KD, et al. Evaluation of a soluble tetrazolium/formazan assay for cell growth and drug sensitivity in culture using human and other tumor cell lines. Cancer Res. 1988; 48:4827–4833. [PubMed: 3409223]

59. Roehm NW, Rodgers GH, Hatfield SM, Glasebrook AL. An Improved colorimetric assay for cell proliferation and viability utilizing the tetrazolium salt Xtt. J Immunol Methods. 1991; 142:257–265. [PubMed: 1919029]

60. Cell Signaling Technology, I.: Xtt Cell Viability Kit. 2011.

61. Boss SD, Betzel T, Muller C, et al. Comparative studies of three pairs of α- and γ-conjugated folic acid derivatives labeled with fluorine-18. Bioconjug Chem. 2016; 27:74–86. [PubMed: 26634288]

62. Fröhlich E. The role of surface charge in cellular uptake and cytotoxicity of medical nanoparticles. Int J Nanomed. 2012; 7:5577–5591.

63. Darzynkiewicz Z, Bruno S, Del BG, et al. Features of apoptotic cells measured by flow cytometry. Cytometry. 1992; 13:795–808. [PubMed: 1333943]

64. Raschke WC, Baird S, Ralph P, Nakoinz I. Functional macrophage cell lines transformed by Abelson leukemia virus. Cell. 1978; 15:261–267. [PubMed: 212198]

65. Arnida A, Janát-Amsbury MM, Ray A, Peterson CM, Ghandehari H. Geometry and surface characteristics of gold nanoparticles influence their biodistribution and uptake by macrophages. Eur J Pharm Biopharm. 2011; 77:417–423. [PubMed: 21093587]

66. Kelly C, Jefferies C, Cryan S-A. Targeted liposomal drug delivery to monocytes and macrophages. Journal of Drug Delivery. 2011; 2011:11.

67. Hong S, Rattan R, Majoros IJ, et al. The role of ganglioside Gm1 in cellular internalization mechanisms of poly(amidoamine) dendrimers. Bioconjug Chem. 2009; 20:1503–1513. [PubMed: 19583240]

68. Rattan R, Vaidyanathan S, Wu GSH, Shakya A, Orr BG, Banaszak Holl MM. Polyplex-induced cytosolic nuclease activation leads to differential transgene expression. Mol Pharm. 2013; 10:3013–3022. [PubMed: 23834286]

69. Goonewardena SN, Zong H, Leroueil PR, Baker JR Jr. Bioorthogonal chemical handle for tracking multifunctional nanoparticles. ChemPlusChem. 2013; 78:430–437.

70. Rostovtsev VV, Green LG, Fokin VV, Sharpless KB. A stepwise Huisgen cycloaddition process: copper(I)-catalyzed regioselective "ligation" of azides and terminal alkynes. Angew Chem Int Ed. 2002; 41:2596–2599.

71. Swirski FK, Libby P, Aikawa E. Ly-6chi monocytes dominate hypercholesterolemia-associated monocytosis and give rise to macrophages in atheromata. J Clin Invest. 2007; 117:195–205. [PubMed: 17200719]

72. Jokerst JV, Lobovkina T, Zare RN, Gambhir SS. Nanoparticle pegylation for imaging and therapy. Nanomedicine. 2011; 6:715–728. [PubMed: 21718180]

73. Knop K, Hoogenboom R, Fischer D, Schubert US. Poly(ethylene glycol) in drug delivery: pros and cons as well as potential alternatives. Angew Chem Int Ed Engl. 2010; 49:6288–6308. [PubMed: 20648499]

74. Knop K, Hoogenboom R, Fischer D, Schubert US. Poly(ethylene glycol) in drug delivery: pros and cons as well as potential alternatives. Angew Chem Int Ed. 2010; 49:6288–6308.

75. Dos Santos N, Allen C, Doppen A-M, et al. Influence of poly(ethylene glycol) grafting density and polymer length on liposomes: relating plasma circulation lifetimes to protein binding. Biochim Biophys Acta, Biomembr. 2007; 1768:1367–1377.

76. Garay RP, Labaune JP. Immunogenicity of polyethylene glycol (Peg). Open Conf Proc J. 2011; 2:104–107.

77. Gaberc-Porekar V, Zore I, Podobnik B, Menart V. Obstacles and pitfalls in the pegylation of therapeutic proteins. Curr Opin Drug Discov Devel. 2008; 11:242–250.

78. Pelegri-O'Day EM, Lin E-W, Maynard HD. Therapeutic protein-polymer conjugates: advancing beyond pegylation. J Am Chem Soc. 2014; 136:14323–14332. [PubMed: 25216406]

79. Schlapschy M, Binder U, Boerger C, et al. Pasylation: a biological alternative to pegylation for extending the plasma half-life of pharmaceutically active proteins. Protein Eng Des Sel. 2013; 26:489–501. [PubMed: 23754528]

80. Styslinger TJ, Zhang N, Bhatt VS, Pettit N, Palmer AF, Wang PG. Site-selective glycosylation of hemoglobin with variable molecular weight oligosaccharides: potential alternative to pegylation. J Am Chem Soc. 2012; 134:7507–7515. [PubMed: 22489605]

81. Barz M, Luxenhofer R, Zentel R, Vicent MJ. Overcoming the Peg-addiction: well-defined alternatives to peg, from structure-property relationships to better defined therapeutics. Polym Chem. 2011; 2:1900–1918.

82. Letelier ME, Lepe AM, Faundez M, et al. Possible mechanisms underlying copper-induced damage in biological membranes leading to cellular toxicity. Chem Biol Interact. 2005; 151:71–82. [PubMed: 15698579]

83. Estephan ZG, Schlenoff PS, Schlenoff JB. Zwitteration as an alternative to pegylation. Langmuir. 2011; 27:6794–6800. [PubMed: 21528934]

84. Shi X, Wang SH, Swanson SD, et al. Dendrimer-functionalized shell-crosslinked iron oxide nanoparticles for in-vivo magnetic resonance imaging of tumors. Adv Mater (Weinheim, Ger). 2008; 20:1671–1678.

85. Gabrielson NP, Pack DW. Acetylation of polyethylenimine enhances gene delivery via weakened polymer/DNA interactions. Biomacromolecules. 2006; 7:2427–2435. [PubMed: 16903692]

86. Majoros IJ, Keszler B, Woehler S, Bull T, Baker JR Jr. Acetylation of poly (amidoamine) dendrimers. Macromolecules. 2003; 36:5526–5529.

87. Shi X, Lee I, Baker JR. Acetylation of dendrimer-entrapped gold and silver nanoparticles. J Mater Chem. 2008; 18:586–593.

A. Supplementary data

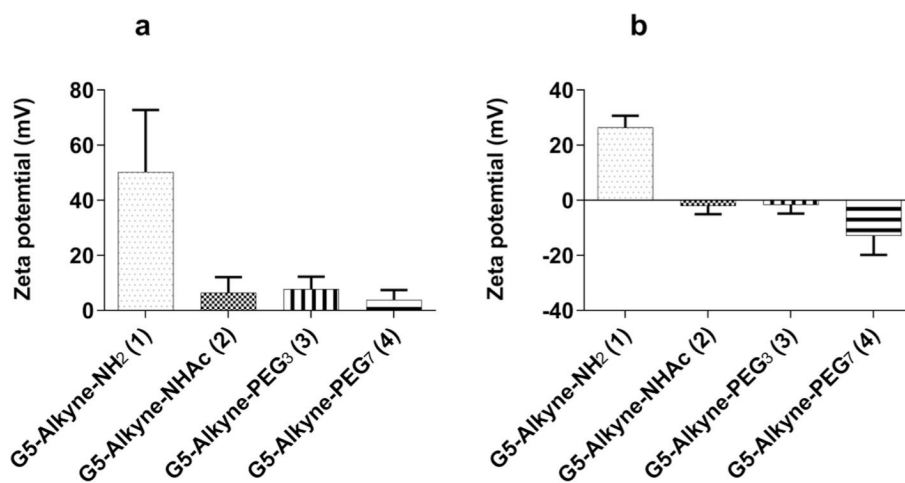Supplementary data associated with this article can be found, in the online version, at http://dx.doi.org/10.1016/j.bmc.2017.06.040.

Fig. 1.
Zeta potential of modified dendrimer conjugates. Zeta potentials for G5-Alkyne-NH$_2$ (1), G5-Alkyne-NHAc (2), G5-Alkyne-PEG$_3$ (3) and G5-Alkyne-PEG$_7$ (4) in Molecular grade water (a) and in 1 mM HEPES pH 7 buffer (b) are shown above. As expected, G5-Alkyne-NH$_2$ (**1**) has the most positive charge. G5-Alkyne-NHAc (**2**), G5- Alkyne-PEG$_3$ (**3**) and G5-Alkyne-PEG$_7$ (**4**) are all similar in charge and are close to neutral in molecular grade water and in 1 mM HEPES pH 7.
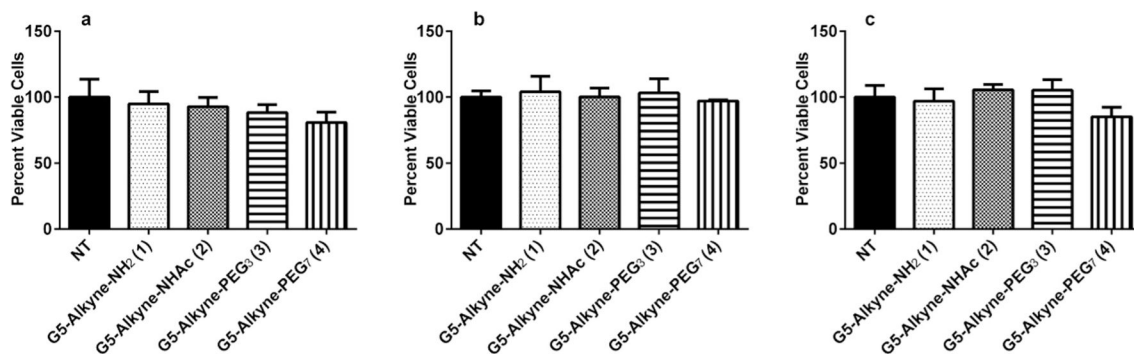
Fig. 2.
Cytotoxicity of the modified dendrimer conjugates in RES cells. RAW264.7 cells were incubated with 100 nM dendrimer conjugates for (a) 2 h, (b) 24 h, and (c) 48 h. Following incubation, cytotoxicity of the dendrimers was assessed using the XTT assay. NT signifies no treatment control. None of the dendrimer conjugates were cytotoxic at the time points evaluated.
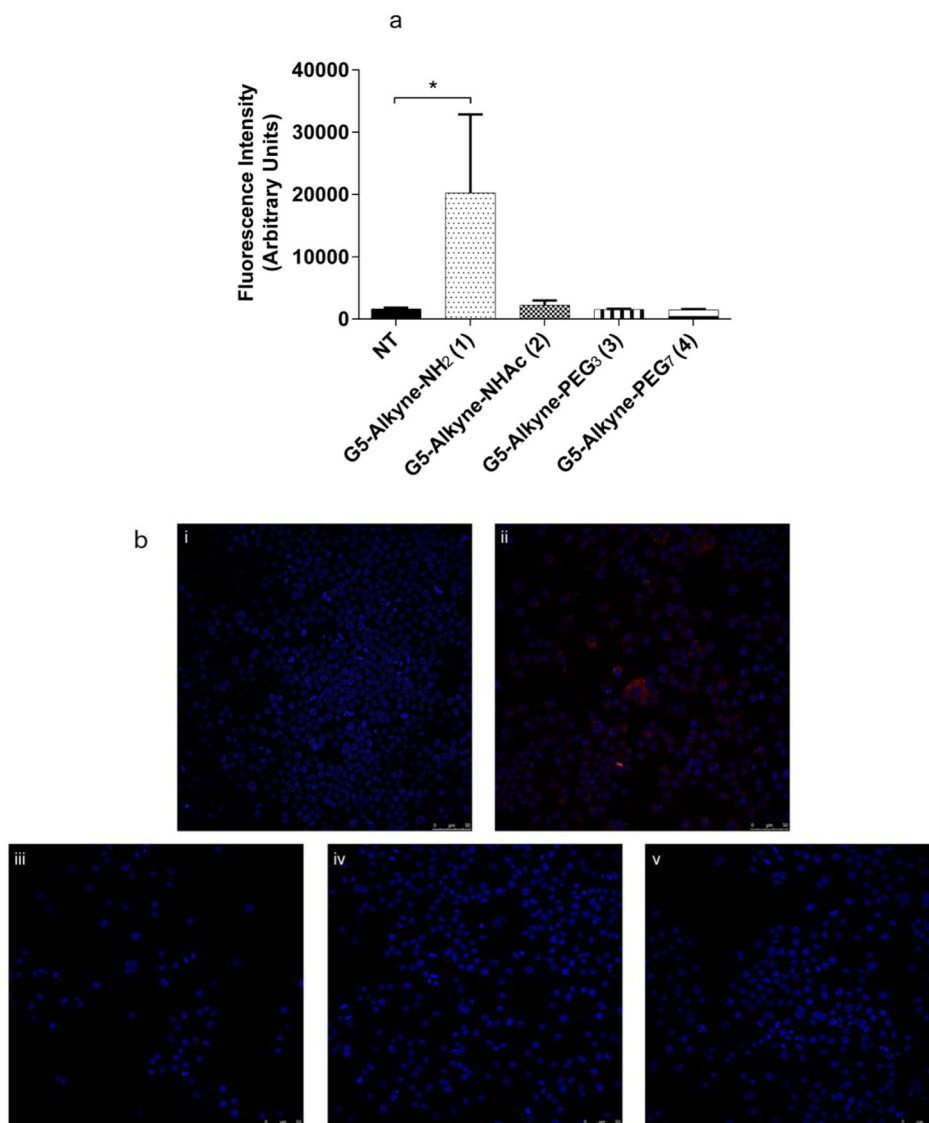
Fig. 3.
Flow cytometry and confocal evaluation of modified dendrimer conjugates clearance in RES cells. A) RAW264.7 cells were incubated with 10 nM of the dendrimer conjugates for 2 h. After incubation, the cells were harvested and AF647 was conjugated in situ using the CuAAC approach. Dendrimer clearance (Fluorescence Intensity) was then measured using flow cytometry. G5-Alkyne-NHAc (**2**), G5-Alkyne-PEG$_3$ (**3**), and G5-Alkyne-PEG$_7$ (**4**) showed minimal clearance by RES cells compared with the unmodified dendrimer (G5-Alkyne-NH$_2$ (**1**)). Asterisk represents statistical difference between (One way Anova, Dunnett's post hoc test, P value <0.05) NT and treatments. B) RAW264.7 cells were incubated with 100 nM of the modified dendrimer conjugates for 2 h. After incubation, the cells were harvested and AF555 was conjugated in situ using the Confocal CuAAC approach. Dendrimer clearance by RES cells was evaluated using confocal microscopy probing for AF555 (NP) and DAPI (cell nuclei) for (i) NT, (ii) G5- Alkyne-NH$_2$ (**1**), (iii) G5-Alkyne-NHAc (**2**), (iv) G5-Alkyne-PEG$_3$ (**3**), and (v) G5-Alkyne-PEG$_7$ (**4**). Again, G5-

Alkyne-NHAc (**2**), G5-Alkyne-PEG$_3$ (**3**), and G5-Alkyne-PEG$_7$ (**4**) showed minimal clearance by RES cells compared with the unmodified dendrimer (G5-Alkyne-NH$_2$ (**1**)). Results are representative of at least 3 independent experiments.
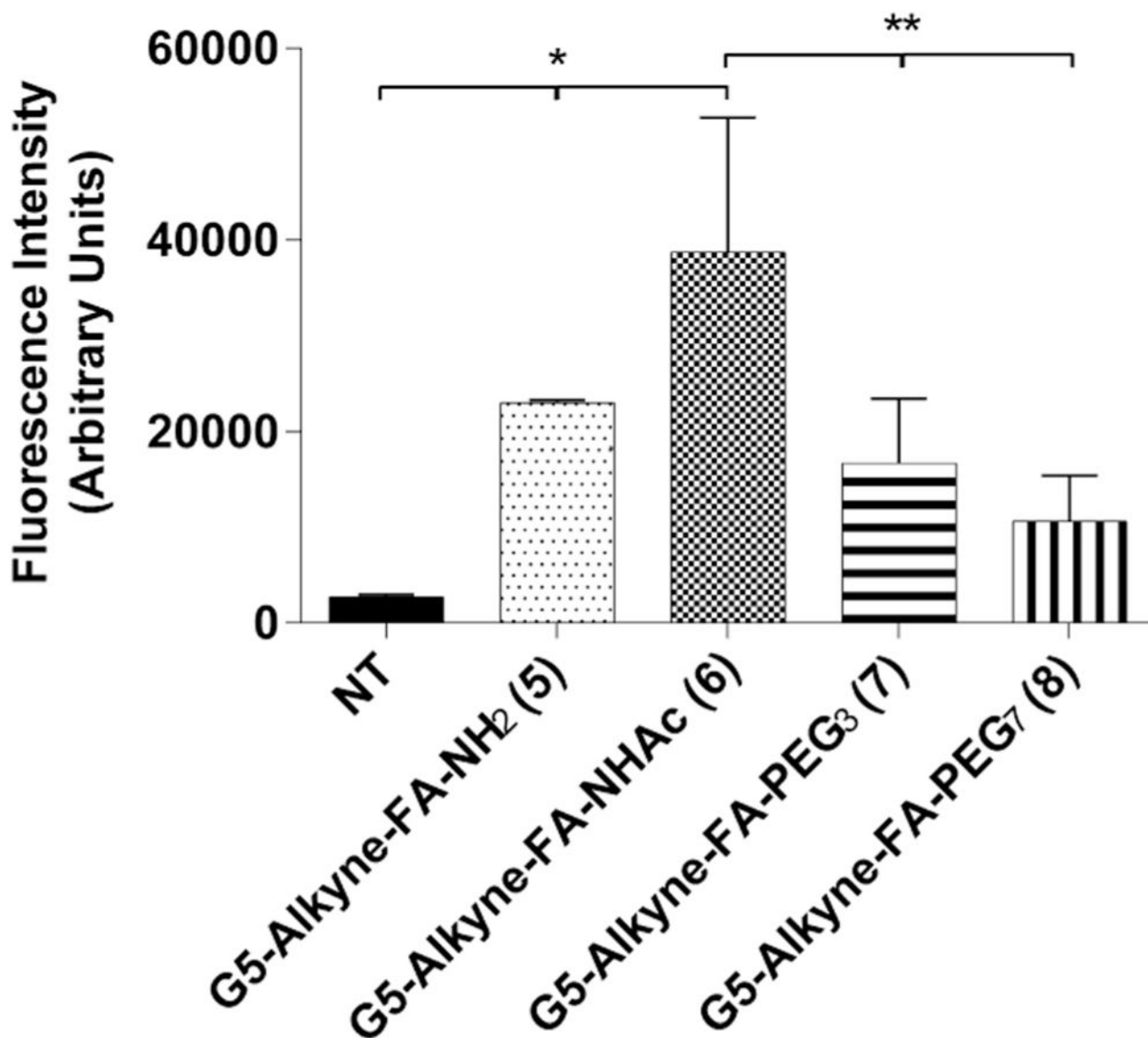
Fig. 4.
Effects of surface modifications on tumor-specific targeting of dendrimer conjugates. KB cells were incubated with 10 nM of the targeted, surface-modified dendrimer conjugates for 2 h. After incubation, the cells were harvested and AF647 was conjugated in situ using the CuAAC approach. Dendrimer uptake was then measured using flow cytometry. Surprisingly, the acetylated targeted dendrimer conjugate (**6**) demonstrated significantly more uptake than both the PEGylated targeted dendrimer conjugates (**7** and **8**). *P < 0.05 for NT and treatments (One way Anova, Dunnett's post hoc test). **P < 0.05 between G5-Alkyne-FA-NHAc (**6**) and other treatments (One way Anova, Dunnett's post hoc test). Results are representative of 3 independent experiments.
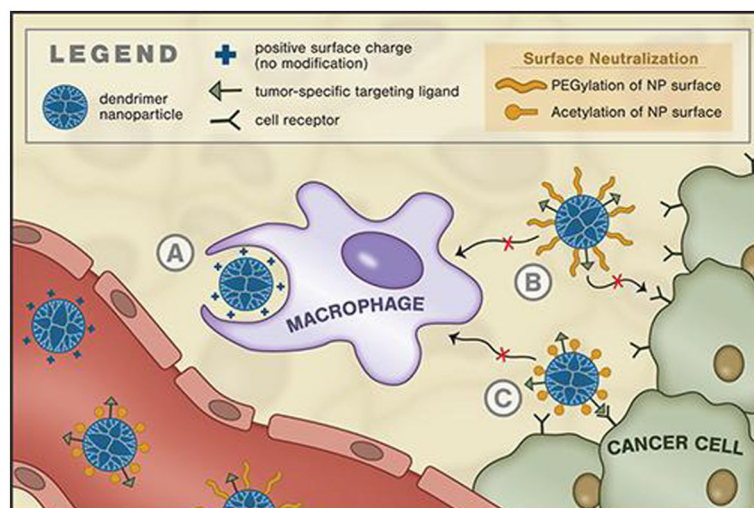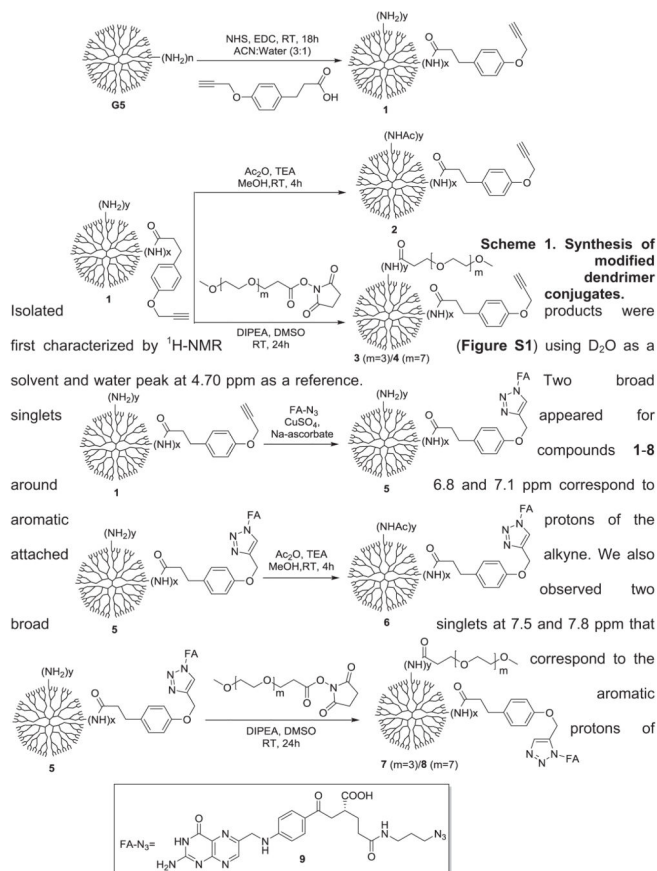
Fig. 5.
Schematic of effects of PEGylation and acetylation of NP surface on RES clearance and tumor-specific targeting. Graphic presentation not to scale.

Scheme 1.
Synthesis of modified dendrimer conjugates.